

Efficient Modelling of Band-Gap and Metamaterial Structures in EMC

Hiroki Wakatsuchi¹, Steve Greedy, John Paul, and Christos Christopoulos²

George Green Institute for Electromagnetics Research, Electrical and Electronic Engineering, University of Nottingham
Tower Building, University Park, University of Nottingham, Nottingham, NG7 2RD, UK

¹hirokiwaka@gmail.com

²Christos.Christopoulos@nottingham.ac.uk

Abstract— The purpose of this research is to present efficient models of novel materials and surfaces based on metamaterials (MTM) and/or electromagnetic band-gap structures (EBG) suitable for large scale simulation in electromagnetic compatibility (EMC) problems. It is shown that the employment of digital filter (DF) techniques provides an efficient means of describing such materials (which inevitably consist of several electrically small components) in a large scale coarse mesh suitable for modelling practical EMC problems. The basic structure of the DF and its embedding into a TLM solver are briefly described together with the derivation of the DF parameters for the EBG and MTM materials.

Key words: Transmission-Line Modelling, TLM, digital filtering technique, electromagnetic band gap material, metamaterial.

I. INTRODUCTION

In recent years significant development in the field of materials has taken place making it possible to obtain materials with properties hitherto not available in nature. The impact of such materials in electromagnetic design has not yet been exploited fully. Some examples of possible applications are: electromagnetic band gap (EBG) structures that make it possible to stop propagation in specific frequency bands [1]; metamaterials (MTM) which possesses negative dielectric and/or magnetic characteristic in certain frequency bands [2, 3]. These new materials are being continuously improved e.g. in the realization of multi-resonances [4]. Now the main interest in the research field of electromagnetic compatibility (EMC) is focused on applications in realistic EMC problems (such as coupling between devices, shielding, etc).

A limiting factor in the wider study of such materials and their impact on EMC design is the difficulty in constructing suitable efficient numerical models which can be used for “what if” studies and their evaluation in practical situations. By their nature, the details of such materials are much smaller than the wavelength and therefore a numerical model directly applied would need a very fine sub-wavelength resolution to reproduce essential geometrical detail. However, large scale simulation in EMC is normally based on a tenth of a wavelength resolution. A finer resolution although possible in principle, would result in a computationally expensive calculation. This is an example of a multi-scale problem which requires special techniques to embed fine features into a coarse global mesh [5]. For example, if an EBG material is modelled using a resolution of 0.1 mm [6], this cell size will simulate waves up to 300 GHz, although most stop bands are

designed to be in the 10 GHz range. Therefore, such simulations are very time-consuming and in many practical cases impossible.

To solve such problems, the digital filtering (DF) technique described in [7, 8] could be used. In applying this method we first obtain the frequency dependent properties of a unit cell of the material under consideration and from this information derive reflection and transmission coefficients which are then converted to a time-domain procedure through the DF technique. This results in a very efficient algorithm which enables us to use large cell sizes and therefore significantly reduce calculation time.

In this paper, the application of the DF technique for an EBG material is presented. First, this paper introduces the modelling method, including overviews of the TLM and DF techniques. Second, the details of the modelled material are explained and calculation results obtained by the conventional method and DF technique are shown. The results are then compared and the main features of the DF approach are discussed.

II. ANALYSIS METHOD

A. Transmission Line Modelling Method

In this paper the TLM method is used to calculate the electromagnetic (EM) field. The TLM method [9, 10, 11] reduces the simulation space to a lumped circuit model, composed of capacitors and inductors. The lumped circuit

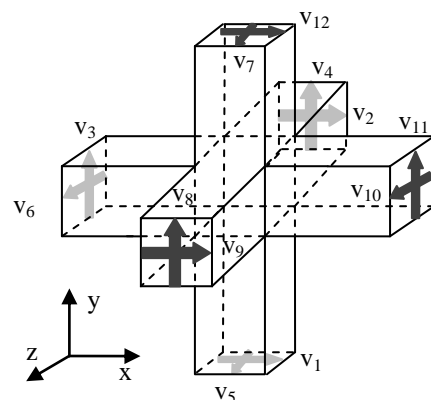


Fig. 1 Unit cell of TLM.

model effectively spatially discretises the problem into nodes or cells that may be replaced by their transmission line equivalents. Each cell has a number of ports and the situation for free space is illustrated in Fig. 1. The inclusion of dielectric and/or magnetic material is accomplished through the addition of extra ports (stubs). In TLM, the procedure to obtain the EM field is composed of four steps. First, the initial condition is given and, second, the voltages scattered from the centre of cell are calculated from Eq. (1).

$$\mathbf{V}^r = \mathbf{S} \cdot \mathbf{V}^i \quad (1)$$

where \mathbf{S} is scattering matrix and superscripts of \mathbf{V} , \mathbf{r} and \mathbf{i} , express the reflected and incident voltages, respectively. For free space modelling, each cell has 12 port voltages ($\mathbf{V} = [v_1 v_2 \dots v_{12}]^T$) and the scattering matrix is:

$$0.5 \begin{bmatrix} 0 & 1 & 1 & 0 & 0 & 0 & 0 & 0 & 1 & 0 & -1 & 0 \\ 1 & 0 & 0 & 0 & 0 & 1 & 0 & 0 & 0 & 0 & -1 & 0 & 1 \\ 1 & 0 & 0 & 1 & 0 & 0 & 0 & 1 & 0 & 0 & 0 & 0 & -1 \\ 0 & 0 & 1 & 0 & 1 & 0 & -1 & 0 & 0 & 0 & 0 & 1 & 0 \\ 0 & 0 & 0 & 1 & 0 & 1 & 0 & -1 & 0 & 1 & 0 & 0 & 0 \\ 0 & 1 & 0 & 0 & 1 & 0 & 1 & 0 & -1 & 0 & 0 & 0 & 0 \\ 0 & 0 & 0 & -1 & 0 & 1 & 0 & 1 & 0 & 1 & 0 & 0 & 0 \\ 0 & 0 & 1 & 0 & -1 & 0 & 1 & 0 & 0 & 0 & 0 & 1 & 0 \\ 1 & 0 & 0 & 0 & 0 & -1 & 0 & 0 & 0 & 0 & 1 & 0 & 1 \\ 0 & -1 & 0 & 0 & 1 & 0 & 1 & 0 & 1 & 0 & 0 & 0 & 0 \\ -1 & 0 & 0 & 1 & 0 & 0 & 0 & 1 & 0 & 0 & 0 & 1 & 0 \\ 0 & 1 & -1 & 0 & 0 & 0 & 0 & 0 & 1 & 0 & 1 & 0 & 0 \end{bmatrix}$$

Third, the new incident voltages are obtained from the reflected voltages entering from neighbouring cells (connection). The second and third processes (scatter and connect) are repeated for as long as required. Finally, the EM field is derived from the incident voltages, using

$$E_{(x, y, z)} = -\frac{v_{(1, 3, 5)}^i + v_{(2, 4, 6)}^i + v_{(9, 11, 7)}^i + v_{(12, 8, 10)}^i}{2\Delta l} \quad (2)$$

$$H_{(x, y, z)} = \frac{v_{(4, 6, 1)}^i + v_{(7, 9, 11)}^i - v_{(5, 2, 3)}^i - v_{(8, 10, 12)}^i}{2Z\Delta l} \quad (3)$$

In these equations Δl is the cell size and Z is the free-space impedance. The scattering matrix and EM field calculation for the cases of dielectric and magnetic materials are reported in [9, 10].

B. Digital Filtering Technique

The DF technique [7, 8] is the method used to convert the frequency domain characteristics into the time domain. As a result, it is possible to incorporate frequency dependence in TLM. Furthermore, by using boundary conditions imposed by the derived DF, larger cell sizes may be used to model systems with sub-cell sized features.

To incorporate the DF technique into the TLM method, first of all, it is assumed that the frequency dependant reflection and transmission coefficients may be approximated by Padé form:

$$F(s) = \frac{\sum_{i=0}^{NP} b_i s^i}{\sum_{i=0}^{NP} a_i s^i} = \frac{b_0 + b_1 s + \dots + b_{NP} s^{NP}}{a_0 + a_1 s + \dots + s^{NP}} \quad (4)$$

where s is the complex frequency, NP is number of poles and the a and b coefficients are real. This equation may be factorized to yield

$$F(s) = \frac{b_{NP}(s - s_{z0})(s - s_{z1}) \dots (s - s_{z(NP-1)})}{(s - s_{p0})(s - s_{p1}) \dots (s - s_{p(NP-1)})} \quad (5)$$

where s_p and s_z respectively express poles and zeros.

To convert this response from the frequency domain to the time domain the bilinear Z-transform is applied to (5). For instance, $(s - s_{zi})$ is transformed to

$$(s - s_{zi}) \xrightarrow{Z} \alpha_{zi} \frac{1 - z^{-1} \beta_{zi}}{1 - z^{-1}} \quad (6)$$

where $\alpha_{zi} = (2 - s_{zi}\Delta t) / \Delta t$, $\beta_{zi} = (2 + s_{zi}\Delta t) / (2 - s_{zi}\Delta t)$. Applying the bilinear Z-transform to (5) gives

$$F(z) = B_0 \prod_{i=0}^{NP-1} \frac{1 - z^{-1} \beta_{zi}}{1 - z^{-1} \beta_{pi}} \quad (7)$$

$$B_0 = b_{NP} \prod_{i=0}^{NP-1} \frac{\alpha_{zi}}{\alpha_{pi}} \quad (8)$$

After some manipulations we obtain

$$F(z) = \frac{\sum_{i=0}^{NP} B_i z^{-i}}{\sum_{i=0}^{NP} A_i z^{-i}} = B_0 + \frac{\sum_{i=1}^{NP-1} B'_i z^{-i}}{1 + \sum_{i=1}^{NP} A_i z^{-i}} \quad (9)$$

$$B'_i = B_i - B_0 A_i \quad (10)$$

Supposing $F(z)$ represents a reflection function, $F(z) = v_{k+1}^i / v_k^r$, then after some algebra, suppressing the k indices, the incident voltage is put in the form

$$v^i = B_0 v^r + \underline{B}' \cdot \underline{X} \quad (11)$$

where

$$\underline{X} = z^{-1} \underline{A}' \cdot \underline{X} + z^{-1} \underline{1}' v^r \quad (12)$$

$$\underline{A}' = \begin{bmatrix} -A_1 & -A_2 & -A_3 & \dots & -A_{NP-1} & -A_{NP} \\ 1 & & & & & \\ & 1 & & & & \\ & & 1 & & & \\ & & & \dots & & \\ & & & & 1 & \end{bmatrix} \quad (13)$$

$$\underline{1}' = [1 \ 0 \ 0 \ \dots \ 0]^t \quad (14)$$

From (10) to (13), by using X and v^t of previous time step, the frequency dependence may be represented in the time domain. The signal-flow diagram to describe Eq. (11) and (12) is shown in Fig. 2. In this paper, the reflection coefficient is obtained by pre-processing using a numerical model having a very fine resolution (i.e. small cell size Δl). The details are described in the next section.

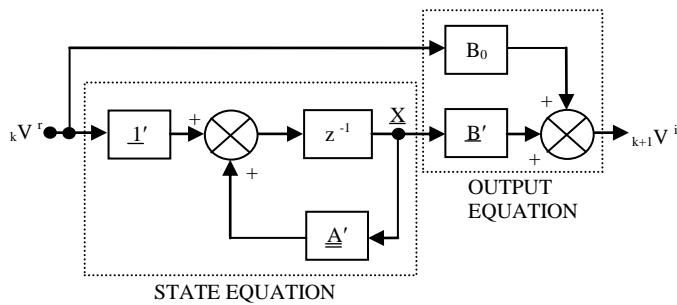


Fig. 2 Signal-flow diagram to calculate new incident voltages between the cells embedding the DF technique.

III. SIMULATION RESULTS

A. Materials

As an example of the application of the DF technique, an EBG structure is simulated. As is shown in Fig. 3, this EBG structure is composed of top plate and bottom plate both connected by a via. The air gap between the two plates is filled with a substrate with relative permittivity $\epsilon_r = 2.2$. The square patch size ($w \times w$) is $4.0 \times 4.0 \text{ mm}^2$ and the diameter of the via, d , was set to be 0.8 mm. Other parameters, h and g , are 1.5 and 0.2 mm, respectively (each symbol corresponding to those in Fig. 3).

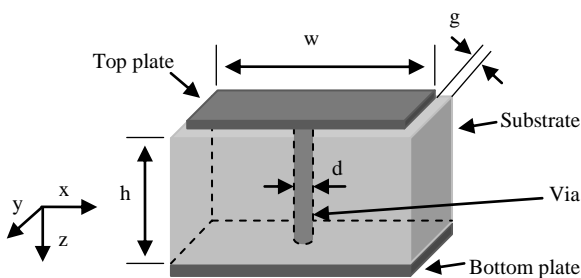


Fig. 3 Simulated EBG structure.

B. Simulation Results

To begin with, the reflection coefficient for a single EBG element is calculated using a fine mesh and the result is converted into Padé form to obtain each constant of Eq. (4). The fine mesh used to model the EBG structure shown in Fig. 3 is comprised of cells of size $0.1 \times 0.1 \times 0.1 \text{ mm}^3$. The analysis space in the xy plane is the same as that of the top plate. In the z direction, 40 cells are used above the top plate and a Gaussian pulse is excited on a plane two cells away from uppermost boundary. In addition, an observation plane to sample the reflected pulse is set to one cell below the excitation plane. The boundary conditions on the xy plane are perfectly matched and all other planes have a periodic boundary condition. In Fig. 4, the complex reflection coefficient is compared with that converted into Padé form, in which the number of poles is two. In Table I, the constants of the Padé form are displayed.

From Fig. 4 and Table I, it is confirmed that in using two poles, the reflection coefficient obtained from the fine-mesh is accurately described after conversion into the Padé form.

The reflection coefficient obtained by the DF technique and that of the fine mesh (the initial reflection coefficient) are compared. To begin with, the result of Fig. 4 is factorized and, then, \underline{A}' , B_0 , and \underline{B}' of Eq. (11) are calculated to decide the boundary condition of the DF. In this calculation, the cell size using the DF implementation is set to $1.0 \times 1.0 \times 1.0 \text{ mm}^3$, which is 10 times that of the initial simulation, yielding a reduction by a factor of a 1000 in the number of cells used to describe the original problem. The comparison result is shown in Fig. 5.

As a result of the application of the DF technique, it is found from Fig. 5 that, when a coarse mesh is applied with the DF simulation, the reflection coefficient shows a close agreement with that of fine mesh. In addition, increasing the cell volume by a factor of a 1000, the simulation to model the EBG structure can be implemented at a fraction of the computational cost of the fine-mesh simulation.

TABLE I
COEFFICIENTS OF EQ. (4) FOR EBG STRUCTURE.

i	a_i	b_i
0	5.50562×10^{21}	-5.49485×10^{21}
1	2.69504×10^{10}	2.59674×10^{10}
2		-0.992844

IV. CONCLUSION

In this paper, the efficient modelling of an EBG structure was presented through application of the DF technique in a TLM simulation. It was shown that by using two poles, the reflection coefficient in the simulated model can be accurately represented. This result was then used to obtain the constants required to embed the DF into coarse mesh TLM. A comparison of the fine-mesh simulation of the EBG element with the coarse-mesh simulation supplemented by the DF model of the EBG boundary shows a very close agreement but

in the latter case at a fraction of the computational cost. This efficient model can be used in large-scale EMC simulations which contain complex EBG surfaces.

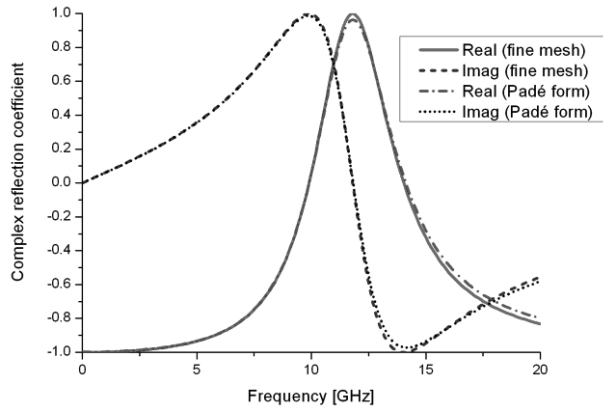


Fig. 4 Complex reflection coefficient in Padé form.

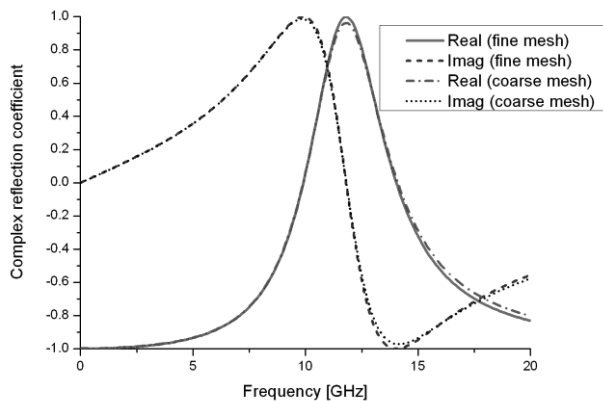


Fig. 5 Complex reflection coefficient in DF simulation.

REFERENCES

- [1] D. F. Sievenpiper, "High-impedance electromagnetic surface," PhD Thesis, Dept. of Electrical Engineering, UCLA, CA, USA, 1999.
- [2] J. B. Pendry, A. J. Holden, D. J. Robbins, and W. J. Stewart, "Magnetism from conductors and enhanced nonlinear phenomena," *IEEE Trans. Microw. Theory Tech.*, vol. 47, pp.2075-2084, Nov. 1999.
- [3] D. R. Smith, W. J. Padilla, D. C. Vier, S. C. Nemat-Nasser, and S. Schultz, "Composite medium with simultaneously negative permeability and permittivity," *Phys. Rev. Lett.*, vol. 84, pp. 4184-4187, May 2000.
- [4] C. M. Bingham, H. Tao, X. Liu, R. D. Averitt, X. Zhang, and W. J. Padilla, "Planar Wallpaper Group Metamaterials for Novel Terahertz Applications," *Opt. Express*, vol. 16, no.23, pp. 18565-18575, 2008.
- [5] C. Christopoulos, "Multi-scale modelling in time-domain electromagnetics," *AEU International Journal of Electronics Communications*, vol. 57, no. 2, pp. 100-110, 2003.
- [6] B. Mohajer-Iravani, S. Shahparnia, and O. M. Ramahi, "Coupling reduction in enclosures and cavities using electromagnetic band gap structures," *IEEE Trans. Electromagn. Compat.*, vol. 48, no. 2, pp. 292-303, May 2006.
- [7] J. Paul, V. Podlozny, and C. Christopoulos, "The use of digital filtering techniques for the simulation of fine features in EMC problems solved in the time domain," *IEEE Trans., Electromagn. Compat.*, vol. 45, pp. 238-244, May 2003.
- [8] J. Paul, V. Podlozny, D. W. P. Thomas, and C. Christopoulos, "Time-Domain Simulation of Thin Material Boundaries and Thin Panels Using Digital Filters in TLM," *Turk. J. Elec. Engin.*, vol. 10, no.2, pp. 185-198, 2002.
- [9] C. Christopoulos, "The transmission-line modeling method: TLM," New York: IEEE Press, 1995.
- [10] P. B. Johns, "A symmetrical condensed node for the TLM method," *IEEE Trans. Trans. Microw. Theory Tech.* vol. 35, no. 4, pp. 370-377, Apr. 1987.
- [11] C. Christopoulos, "The transmission-line modeling (TLM) method in electromagnetics," USA: Morgan & Claypool Publishers series, 2006.